Catalysis Today 168 (2011) 57–62

Contents lists available at ScienceDirect

Catalysis Today

journal homepage: www.elsevier.com/locate/cattod

Characterization of the pore architecture created by alkaline treatment of HMCM-22 using ^{129}Xe NMR spectroscopy

A. van Miltenburg[a,*,1], L.C. de Ménorval[b,*], M. Stöcker[a]

[a] SINTEF Materials and Chemistry, PO Box 124, Blindern, 0314 Oslo, Norway
[b] Institut Charles Gerhardt Montpellier, UMR-5253 CNRS-UM2, Equipe Agrégats, Interface, et Matériaux pour l'Energie, Université Montpellier 2, CC-1502, Place Eugène Bataillon, 34095 Montpellier Cedex 5, France

ARTICLE INFO

Article history:
Received 6 October 2010
Received in revised form 16 January 2011
Accepted 17 January 2011
Available online 26 February 2011

Keywords:
Desilication
HMCM-22
^{129}Xe NMR spectroscopy

ABSTRACT

The pore architecture of alkaline treated HMCM-22 zeolite was investigated by ^{129}Xe NMR spectroscopy. The spectra show that additional porosities have been formed after the alkaline treatment. Up to a treatment with 0.20 M NaOH new micropores are formed which gradually grow in size to the mesoporous range at higher alkaline treatment conditions. Furthermore, interconnections between the two independent channel systems are formed, leading to an increase in the porosity and a further evolution of the porosity towards the mesoporous range. The results are in accordance with earlier characterization and catalytic results and conclusions drawn in our previous study.

1. Introduction

Zeolites are attractive materials for various catalytic reactions, because of their large surface areas, thermal stability and shape selective pore structure. Unfortunately, in the practical industrial process some drawbacks of the microporous structure may appear. Often reactions are largely affected by mass-transfer/diffusion limitations. Although the small zeolite pores of similar sizes as the molecules make a selective transport of reactants and/or products possible, this diffusional transport is usually very slow ($D < 10^{-8}$ m^2 s^{-1}). These limitations are more pronounced in case of large zeolite crystals or two-dimensional pores in slab-like zeolite crystals. In order to enhance this transport, one can introduce additional mesoporosity into the pore systems, which results in a shorter effective diffusion length. Several research groups have investigated various ways of introducing this additional mesoporosity into the system, either by using a modified synthesis, or by post-synthesis treatments [1–4].

The MCM-22 zeolite (IZA Code MWW) [5,6] consists of two non-interconnecting channel systems: a two-dimensional 10-ring sinusoidal channel system (0.41 nm × 0.51 nm), and a two-dimensional straight 10-ring (0.41 × 0.55 nm) interlayer pore system. This interlayer pore contains 12-ring side pockets (with inner diameter of 0.71 nm and height of 1.82 nm), resulting in large cavities. MCM-22 is an industrially attractive catalyst for benzene alkylation with ethylene or propylene [7,8].

In a previous study [9] we modified the HMCM-22 zeolite (with a Si/Al-ratio of 17) via a post-synthesis alkaline treatment to create an interconnected micro/meso-porous pore system. It was shown that, although a partial destruction of the zeolite framework occurred, additional porosity was formed and an interconnection between the two independent pore structures of MCM-22 was created. Concerning the Si/Al-ratio, it should be noted that Groen et al. [10] showed that the desilication process for a ZSM zeolite is most effective, though not limited to, a Si/Al-ratio of 25–50. Therefore, a MCM-22 zeolite with the highest Si/Al-ratio was chosen in our study, i.e. a Si/Al-ratio of 17. Syntheses with higher Si/Al-ratio were not (yet) successful, possibly because a lower Al-content complicates either the formation of the MCM-22 monolayers (MCM-56) or affect the combination of these layers to the layered structure of MCM-22.

In the current study, the change in the pore sizes of several of the alkaline modified HMCM-22 samples are investigated in a qualitative way using ^{129}Xe NMR spectroscopy. The results are compared with the other characterization and catalytic results, presented in our earlier studies [9].

^{129}Xe NMR spectroscopy is now a routine technique for the characterization of porous materials. At the beginning, applications of ^{129}Xe NMR to pore systems have concentrated mostly on studies of crystalline porous materials such as zeolites, and zeolite precursors, related molecular sieves, metal or organic molecules adsorbed in zeolites, and mineral clays [11–21]. Then, a limited number of stud-

* Corresponding authors. Tel.: +31 467223197.
E-mail addresses: Arjen.Miltenburg.van@SABIC-Europe.com (A. van Miltenburg), LCdeMenorval@univ-montp2.fr (L.C. de Ménorval).
[1] Current address: SABIC Europe, PO Box 319, 6160 AH Geleen, The Netherlands.

0920-5861/$ – see front matter © 2011 Elsevier B.V. All rights reserved.
doi:10.1016/j.cattod.2011.01.041

Table 1
Textural properties of the parent and modified HMCM-22 samples obtained by nitrogen sorption [9].

Sample name	C_{NaOH} (mol l^{-1})	A_{BET} (m^2 g^{-1})	V_{micro} (cm^3 g^{-1})	V_{meso} [a] (cm^3 g^{-1})	V_{total} [b] (cm^3 g^{-1})
Parent	–	501	0.149	0.478	0.647
L005	0.05	523	0.179	0.854	1.030
L010	0.10	618	0.209	0.920	1.129
L020	0.20	551	0.187	0.883	1.070
L030	0.30	441	0.148	0.843	0.991
L040	0.40	294	0.100	0.710	0.810
L050	0.50	239	0.081	0.689	0.770

[a] $V_{meso} = V_{total} - V_{micro}$.
[b] Total volume for pores below $p/p_0 = 0.99$.

ies on either amorphous or highly disorder porous systems have been reported [22–25].

The main advantage of the ^{129}Xe NMR is the very high sensitivity of the chemical shift to the local environment of the Xe atom, making it, as the best NMR probe for the porosity studies. The main obstacle in using ^{129}Xe for structural characterization lies in the fact that the observed chemical shift is often dynamically averaged among various xenon environments and therefore cannot be directly related to a specific location. It is necessary to analyse all of the contributions of the observed chemical shift to understand the system.

In a general way, when we try to study chemically modified porous materials we need to briefly describe the theoretical locations of the different possible porosities. The observed ^{129}Xe NMR signal for adsorbed xenon (δ_{obs}) is the weighted average among the different environments sampled by a xenon atom on the NMR time scale:

$$\delta_{obs} = \delta_0 + \delta_S + \delta_{Xe-Xe} + \delta_X$$

where δ_0 is the reference chemical shift of xenon gas at zero pressure (usually set to zero ppm). The δ_S term is the contribution due to the interactions of xenon to the pore surface. These interactions depend on the size of the pores [17–21]. For small pores, the value of δ_S is large as the pore size is smaller, while for larger pores (mesopores), δ_S becomes smaller. Also, δ_S is sensitive to the adsorption of xenon on strong adsorption sites [26]. δ_{Xe-Xe} arises from Xe–Xe collisions and is expected to vary with xenon pressure, or concentration, only for micropores and small mesopores [11,22]. δ_X is a term that takes into account the shift due to the electrical field caused by cations or electrical impurities due to defects on the materials, or the effect of paramagnetic species on the observed material [27].

There is a linear relation between the chemical shift of xenon and the xenon pressure (or concentration) on NaY zeolite [11]. The extrapolation to zero xenon pressure gives us the term δ_S, and the slope is given by the δ_{Xe-Xe} interactions. For HZSM-5 zeolites [27], there is a linear relation between the chemical shift of xenon and the xenon pressure at high Xe pressures. But for low Xe pressures, a minimum for the chemical shift was observed, which then increases sharply (similarly as for the line width) as the pressure decreased further. Here we cannot obtain the term δ_S.

For mesoporous materials [22], the Xe adsorption isotherm is linear, and in contrast to zeolites, the chemical shift of adsorbed Xe is practically independent of the Xe pressure.

In the case of zeolite HMCM-22 [28,29], at low Xe pressures there is a linear relation between the chemical shift of xenon and the xenon pressure (or concentration). At high xenon pressures we can obtain the term δ_{Xe-Xe}, and at low xenon pressure (by extrapolating at zero pressure) we can obtain the term δ_S.

2. Experimental

HMCM-22 (Si/Al = 15) was synthesized according to the earlier described recipe [9]. To obtain a large uniform sample, multiple synthesis batches were combined into a large stock. The HMCM-22 stock was modified via alkaline treatment. Therefore, HMCM-22 crystals (5–10 g) were suspended in a 0.05, 0.10, 0.20, 0.30, 0.40 or 0.50 M solution of sodium hydroxide (NaOH) at 323 K (90 ml solution per gram HMCM-22). After 45 min the suspensions were diluted with ice-cooled water and the solids were separated via centrifugation, followed by three washing steps with ice-cooled water. After drying overnight at room temperature, a two-fold ion-exchange with a 2.0 M aqueous solution of NH_4NO_3 was performed, followed by calcination for 10 h at 813 K (heating rate 2 K min^{-1}). Thereafter the samples were stored and, depending on the applied NaOH concentration, labelled as L005 L010, L020, L030, L040 or L050, respectively. The porous properties of these (modified) samples are summarized in Table 1 and the corresponding X-ray diffraction patterns are shown in Fig. 1 [9].

Powder samples were inserted in special NMR tubes (10 mm o.d.) equipped with a valve. Each sample was first loaded up to a height of about 20 mm, next evacuated for 1 h at room temperature, and then heated at 573 K under vacuum (10^{-3} Pa) during 10 h. Finally the samples were equilibrated at room temperature to a known pressure of xenon (P_{Xe} between 0.5 and 133 kPa).

^{129}Xe NMR spectra were acquired at 297 K using a Bruker AC 250L NMR spectrometer operating at a Larmor frequency of 69.19 MHz. Chemical shifts were referenced with respect to the ^{129}Xe gas resonance ($\delta = 0$ ppm), corrected to the zero density limit

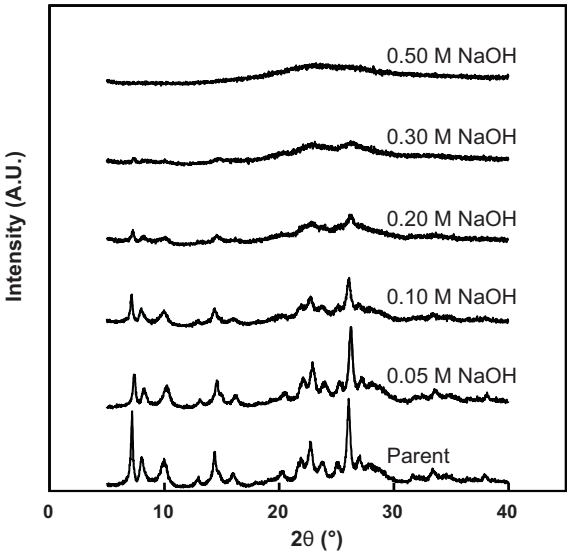

Fig. 1. X-ray diffraction patterns of HMCM-22 treated at 323 K with different alkaline concentrations for 45 min and the parent HMCM-22 [9].

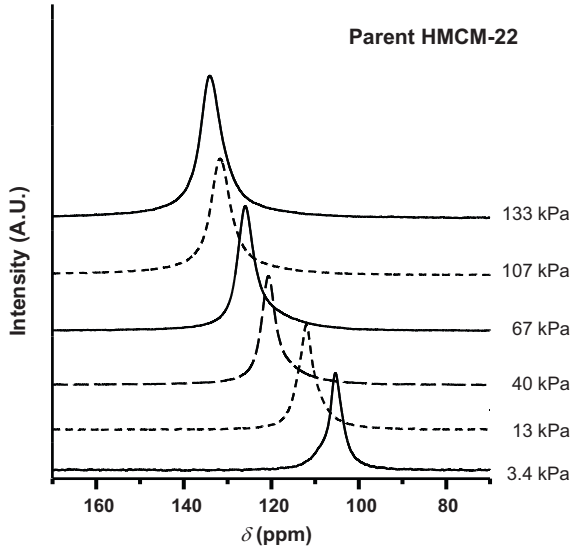

Fig. 2. ^{129}Xe NMR spectra at different xenon pressures for parent HMCM-22.

[30]. Chemical shifts measurements are precise within 0.5 ppm. Block decay spectra were acquired with a recycle delay of 0.5 s between $\pi/2$ pulses. Sample spinning and field locking were not used. Typically 20,000–30,000 signal acquisitions were accumulated for each spectrum.

3. Results and discussion

The ^{129}Xe NMR spectra of the parent sample and modified alkaline treatments (L005, L010 and L020) are presented in Figs. 2–5 for various Xe pressures. The parent HMCM-22 sample (Fig. 2) shows only a single, symmetrical resonance peak, whose chemical shift (ranging from 100 to 140 ppm), shift to low magnetic field with increasing xenon pressure. This implies that only one porosity (the large supercages with 12-ring side pockets) can adsorb xenon in this parent sample [28,29]. Under these conditions, xenon cannot penetrate into the 10-ring porosity, otherwise we should have observed another resonance at a higher chemical shift. The porosity of the 10-ring channels is smaller than those leading to the supercages [17–21,28].

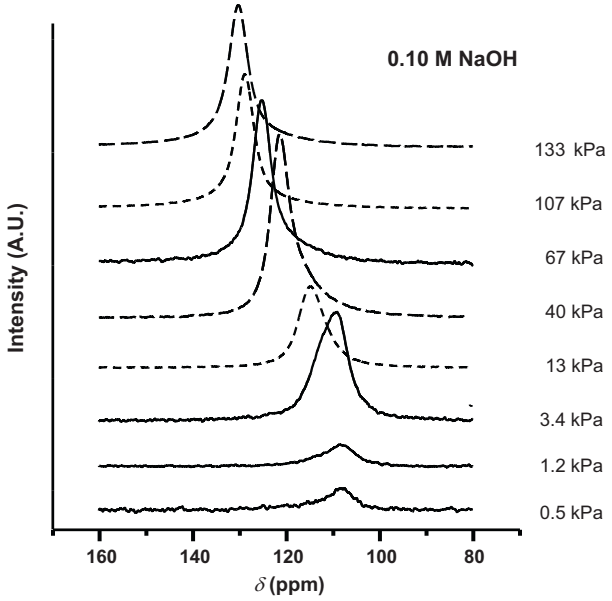

Fig. 4. ^{129}Xe NMR spectra at different xenon pressures for HMCM-22 treated at 323 K with 0.10 M NaOH for 45 min (sample L010).

In Fig. 6, the chemical shift of adsorbed Xe is plotted versus the Xe pressure for the parent sample and samples L005, L010, and L020. For the parent sample, the chemical shift of Xe adsorbed in the supercages with 12-ring side pockets increases as the Xe pressure increases (Fig. 6). There are more and more Xe atoms present in the supercages and thus increase the contribution of Xe–Xe interactions. This means, that the contribution of Xe–Xe interactions to the total ^{129}Xe chemical shift increases.

For the HMCM-22 sample treated with 0.05 M NaOH (sample L005, Fig. 3) at the pressure of 133 kPa, we can only observe one Xe resonance. The obtained value of this resonance is lower compared to the value for the parent sample. This difference corresponds to decreasing Xe–Xe interactions in the porosity of sample L005 relatively to the parent sample. This latter resonance is separated

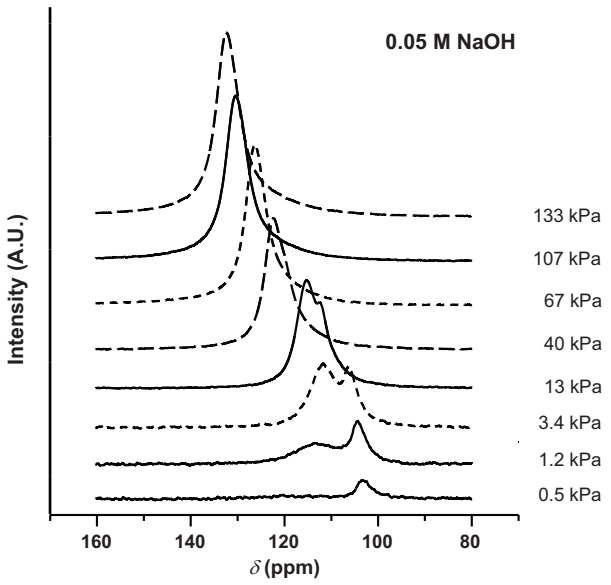

Fig. 3. ^{129}Xe NMR spectra at different xenon pressures for HMCM-22 treated at 323 K with 0.05 M NaOH for 45 min (sample L005).

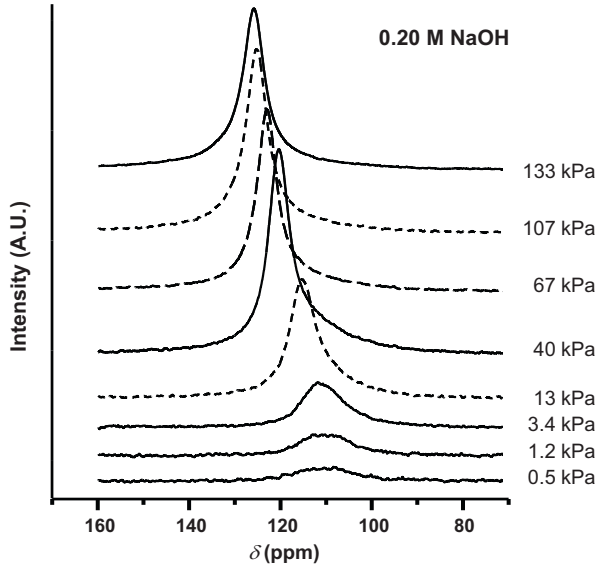

Fig. 5. ^{129}Xe NMR spectra at different xenon pressures for HMCM-22 treated at 323 K with 0.20 M NaOH for 45 min (sample L020).

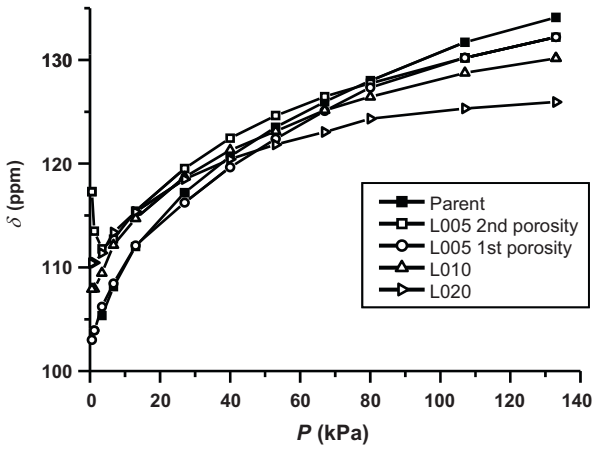

Fig. 6. Chemical shift of ^{129}Xe versus xenon pressure for the main peaks ascribed to the porosities in parent HMCM-22 and HMCM-22 treated at 323 K with 0.05 M, 0.10 M or 0.20 M NaOH for 45 min.

into two resonances (line-1 and line-2), for xenon pressures lower than 80 kPa. The second resonance (line-2), is located at a higher chemical shift than the one related to the supercages (line-1). The second resonance (line-2) has also a non linear pressure dependence with the Xe chemical shift (Fig. 6), for much lower xenon pressures (lower than 3.4 kPa), the Xe chemical shift increases again and the line width becomes much larger than for line-1. This shift is due to electrical impurities which can be ascribed to defects, for instance from extra framework aluminium or additional Lewis sites [9], that were formed during the desilication on the L005 sample [27]. This second resonance can be ascribed to a second porosity in the modified HMCM-22 sample. The observation that for high xenon pressures only one resonance is seen is an indication that the xenon atoms move, within the NMR time scale, in both porosities and thus indicates that these porosities are interconnected. At lower Xe pressures, the two observed resonances possess different chemical shifts. This means that now Xe can be located in two different environments, i.e. two kinds of porosities. One of the porosities corresponds to Xe adsorbed in the supercages with 12-ring side pockets, like for the parent sample. The second one corresponds to a porosity coming from the supercages where some of the atoms are removed from its structure by the desilication treatment and breaking into the 10-ring sinusoidal channels and thus forming porosities where xenon can move inside within the time scale of NMR. As shown in the textural properties (Table 1), the desilication leads to an increase in the mesoporosity of the sample. Furthermore X-ray diffraction shows a partial destruction of the framework. These different characterizations give us the idea that the two porosities are placed in an intragranular mesoporosity environment and this is why at high Xe pressure the Xe–Xe interactions decrease.

Increasing the severity of the alkaline treatment further to 0.10 M NaOH (sample L010, Figs. 4 and 6), results in only one resonance peak in the ^{129}Xe NMR spectra for the different xenon pressures, showing a non linear pressure dependence with the Xe chemical shift. Compared to the parent and L005 samples (line-1), the chemical shift at high xenon pressures has again decreased, indicating that the size of the porosities is still increasing (less Xe–Xe interactions). At lower pressures (<40 kPa) the chemical shift of the resonance of the sample L010 increases relatively to sample L005 (line-1). The existence of only one resonance peak under these conditions indicates that now more and more atoms are removed by desilication from the structure of the 12-ring side-pockets in the supercages, thereby forming connections with the 10-ring sinusoidal channels and thus forming a higher quantity of porosities where xenon can move inside within the time scale of NMR. The NMR resonance peak ascribed to the parent sample has now completely disappeared. The new porosity is formed by a combination of porosities coming from the interconnected 12-ring side pockets (as part of the supercages as well as external cups) and the 10-ring sinusoidal channels. These observations are more pronounced for the HMCM-22 samples treated with 0.20 M NaOH (sample L020, Figs. 5 and 6). That sample shows a non linear relation between the ^{129}Xe NMR chemical shift and xenon pressure, but less accentuated. For high xenon pressures, the Xe chemical shift is again less pronounced, and for low xenon pressures the chemical shift has increased relatively to sample L010.

In summary, our results obtained using ^{129}Xe-NMR for the parent sample up to sample L020, suggest that the porosities of the HMCM-22 changes, leading to interconnected porosities. There is at high xenon pressures a decrease in the δ_{Xe-Xe} chemical shift, and at low xenon pressure an increase in the chemical shift due to the interconnected different microporosities in the framework. The disappearance of the characteristic X-ray diffraction peaks (Fig. 1) for the HMCM-22 zeolite treated with various NaOH concentrations indicates a destruction of more and more of the zeolite framework and thus the disappearance of the characteristic MCM-22 porosities. Also in our earlier study [9], deconvolution of ^{29}Si MAS-NMR spectra indicated a preferential destruction of those Si-atoms located in the bottom of the 12-ring side pockets (both inside the supercages as well as in the external cups) and forming the separation between the two independent 2-dimensional pore systems. These extractions thus lead to the forming of a connection between the two pore systems. The textural properties shown in Table 1 for the parent and treated alkaline HMCM-22 materials confirm the formation of additional porosity up to an alkaline treatment of about 0.10–0.20 M NaOH. At 0.20 M NaOH or above the porosities start to decrease, though the decrease in micropore volume goes much faster than the mesopore volume, reaching a micropore volume much lower than that of the parent MCM-22 sample. From these results we can suggest that we are forming new pores and are creating larger pores. The initial microporosity, mainly coming from the narrower 2-dimensional 10-ring sinusoidal channel system, and the interlayer pore system that contains supercages with 12-ring side pockets (in which xenon can initially be adsorbed), is modified by the alkaline treatment. The alkaline modification leads to an extraction from the framework of some Si atoms, thus opening the porosities of the 10-ring channels, making an interconnection between the interlayer and intralayer (containing the supercages) pore systems. Now xenon can be adsorbed in these new interconnected porosities. As the alkaline treatment becomes stronger and stronger (sample L020 and above), there is a large extraction of Si atoms, and the resulting larger porosity is again a merger of modified pores coming from the initial zeolite structure. The observation of only one resonance (sample L020), is an indication that the xenon atoms move, within the NMR time scale, in the merger of interconnecting modified pores, incorporating the mesoporosities created by desilication.

Increasing the severity of the alkaline treatment further to 0.30–0.50 M NaOH (samples L030, L040 and L050, Figs. 7–9) results again, for the L030 sample, in only one resonance peak in the ^{129}Xe NMR spectra for the different xenon pressures. The chemical shift as a function of the Xe pressure becomes now practically constant (Fig. 10). There are practically no Xe–Xe interactions at high Xe pressure, and at low Xe pressure there is a relatively low decrease in the shift. The interconnected channels have more and more contribution from the now opened 10-ring sinusoidal channels. The desilication process continues to destroy parts of the zeolite framework, creating a lot more holes, and Xe obviously can be adsorbed also in these accessible mesoporosities. The actual porosity is then a merger of porosities coming from the supercages, interconnect-

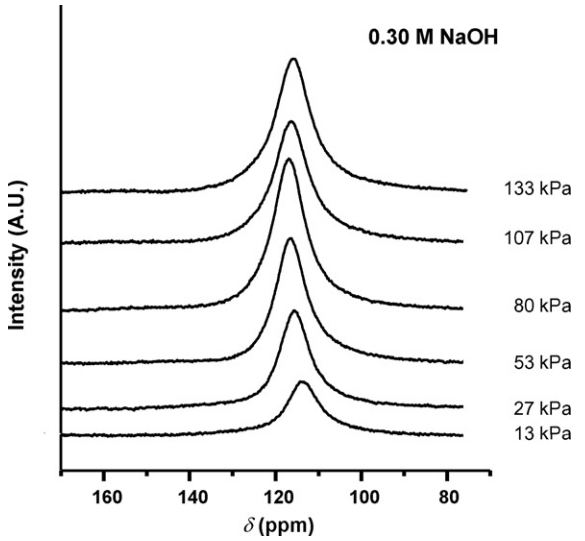

Fig. 7. ^{129}Xe NMR spectra at different xenon pressures for HMCM-22 treated at 323 K with 0.30 M NaOH for 45 min (sample L030).

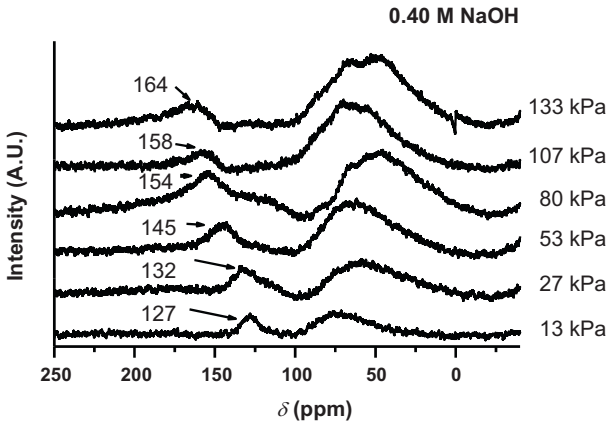

Fig. 8. ^{129}Xe NMR spectra at different xenon pressures for HMCM-22 treated at 323 K with 0.40 M NaOH for 45 min (sample L040).

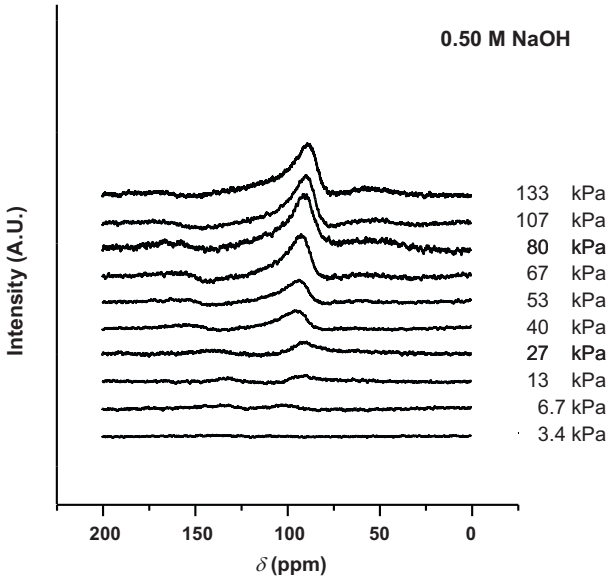

Fig. 9. ^{129}Xe NMR spectra at different xenon pressures for HMCM-22 treated at 323 K with 0.50 M NaOH for 45 min (sample L050).

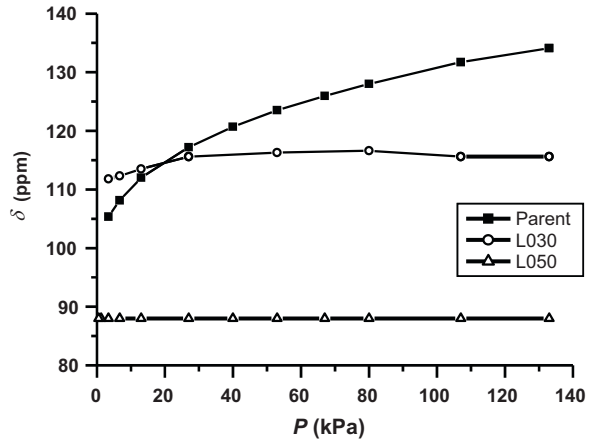

Fig. 10. Chemical shift of ^{129}Xe versus xenon pressure for the main peaks ascribed to the porosities in parent HMCM-22 and HMCM-22 treated at 323 K with 0.30 M or 0.50 M NaOH for 45 min.

ing 10-ring sinusoidal channels, and newly created mesoporosity by the desilication process.

For the L040 sample, we can see the appearance of two different resonances (Fig. 11). The first one (ranging from 120 to 164 ppm) shows an increasing chemical shift with increasing Xe pressures. In the full range, its chemical shift is larger relatively to the resonance peak of the parent sample. We can assign this resonance to adsorbed Xe in 10-ring sinusoidal channels where some Si-atoms of its structure were removed from the zeolite framework during desilication, forming porosities where xenon can move inside within the time scale of NMR. This porosity is independent of the porosity made by the interconnected supercages and side pockets with the 10-ring sinusoidal channels and the mesoporous empty space seen before. Taking into account that the chemical shift of a microporous system depends on the pore size [17–21], we can state that the microporosity of 10-ring sinusoidal channels is smaller than those initially observed for the supercage (with side pockets) pore system in the parent sample.

The second resonance found for the L040 sample, with a broad line width and of which the chemical shift is independent on the Xe pressure (Fig. 11), has a chemical shift value of 58 ppm and corresponds to the mesoporous porosity [22]. Here 10-ring sinusoidal channels, supercages and a lot of empty spaces are connected together into one large pore created by the alkaline treatment of the sample. The zeolite crystals or the aggregates of crystals situ-

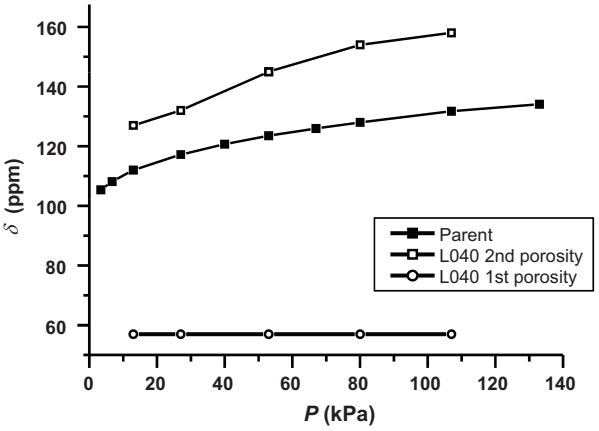

Fig. 11. Chemical shift of ^{129}Xe versus xenon pressure for the main peaks ascribed to the porosities in parent HMCM-22 and HMCM-22 treated at 323 K with 0.40 M NaOH for 45 min.

ated in the intergranular particles are progressively destroyed. Xe can move and has interactions not only with the 10-ring sinusoidal channels and the supercages (partly destroyed) but also with large volume created by desilication, leading to a decrease in the global chemical shift.

For the L050 sample, for all pressures the slope of the line (Fig. 10) is zero, indicating no Xe–Xe interactions and less adsorption of xenon. The obtained chemical shift of this very large resonance is 88 (±10 ppm). Here again the main resonance seen in the spectra corresponds to Xe adsorbed in 10-ring sinusoidal channels (partly destroyed), supercages (partly destroyed) and a mesoporosity due to a destroyed part of the zeolite sample, but now the chemical shift has decreased relatively to the resonance seen in the L040 sample. This means that mesoporosities can evolve as a function of the alkaline attack of the sample, giving a different average of the chemical shift.

From the X-ray diffraction pattern of the HMCM-22 zeolite (Fig. 1), we can see that after alkaline treatment above 0.30 M NaOH the characteristic diffraction lines completely disappear, indicating a severe destruction of the zeolitic crystallinity. The textural properties obtained by nitrogen sorption (Table 1) confirm that parts of the microporous structure are destroyed. These observations and explanations also confirm our conclusions in our previous catalytic study in toluene disproportionation [9]. A treatment at low NaOH concentrations results in a increase of the catalytic activity due to the formation of additional pores, while at too high NaOH concentrations, the catalytic activity decreased due to (partial) destruction of the active sites, i.e. the internal supercages and external half-cups of the HMCM-22 zeolite.

All these experiments suggest that the 10-ring interlayer pore system and the 12-ring side pockets (both within the supercages as well as the external cups) of the MCM-22 zeolite are progressively destroyed, forming larger microporous and mesoporous empty spaces. At the highest applied alkaline treatment (0.50 M NaOH, sample L050), the resulting porosity is a merger of enlarged micropores and a lot of empty spaces. The obtained value of the chemical shift (58 ppm) for the L040 sample (Fig. 8) and for the L050 sample (Fig. 9, 88 ppm) is in accordance with these new porosities. We can also suggest that these new porosities are definitely mesoporous. These mesoporosities should be an intragranular mesoporosity, in the case of sample L050, since for external (or intergranular) empty space, the chemical shift needs to decrease much more (sample L040) [22,23], i.e. xenon is diffusing among larger micropores, internal empty space and external intergranular space.

4. Conclusions

The changes in pore sizes, and the formation of larger (meso)pores were confirmed with ^{129}Xe NMR spectroscopy and are in accordance with earlier characterization and catalytic results obtained and conclusion drawn in our previous study. ^{129}Xe NMR spectroscopy showed the formation of smaller new porosities and interconnections which gradually grow in size and relative quantity after treatment with higher NaOH concentrations. Below a treatment with 0.20 M NaOH, this results in an increase in the micropore volume, creating interconnections between the two independent channel systems, compared to the parent HMCM-22 zeolite. Above a treatment with 0.30 M NaOH, the interconnection to the channel systems increases and new porosities are formed, including the space created by the severe destruction of the zeolite by alkaline treatments. These porosities are in the range of mesoporosity.

Acknowledgements

The authors would like to thank the Marie Curie Research Training Network INDENS (EU FP6 project no: MRTN-CT-2004-005503), and the Network of Excellence INSIDE-POReS (EU FP6) for financial support.

References

[1] J.C. Groen, L.A.A. Peffer, J.A. Moulijn, J. Pérez-Ramírez, Chem. Eur. J. 11 (2005) 4983–4984.
[2] V. Meynen, P. Cool, E.F. Vansant, Micropor. Mesopor. Mater. 104 (2007) 26–38.
[3] C.J.H. Jacobsen, C. Madsen, J. Houzvicka, I. Schmidt, A. Carlsson, J. Am. Chem. Soc. 122 (2000) 7116–7117.
[4] P. Prokešová, S. Mintova, J. Čejka, T. Bein, Mater. Sci. Eng. C 23 (2003) 1001–1005.
[5] Ch. Baerlocher, L.B. McCusker, Database of Zeolite Structures, 2008, http://www.iza-structure.org/databases.
[6] M.E. Leonowicz, J.A. Lawton, S.L. Lawton, M.K. Rubin, Science 264 (1994) 1910–1913.
[7] M.A. Asensi, A. Corma, A. Martinez, J. Catal. 158 (1996) 561–569.
[8] J. Čejka, A. Krejči, N. Žilková, J. Kotrla, S. Ernst, A. Weber, Micropor. Mesopor. Mater. 53 (2002) 121–133.
[9] A. van Miltenburg, J. Pawlesa, A.M. Bouzga, N. Žilková, J. Čejka, M. Stöcker, Top. Catal. 52 (2009) 1190–1202.
[10] J.C. Groen, J.C. Jansen, J.A. Moulijn, J. Pérez-Ramírez, J. Phys. Chem. B 108 (2005) 13062–13065.
[11] T. Ito, J. Fraissard, J. Chem. Phys. 76 (1982) 5225–5229.
[12] L.C. de Ménorval, T. Ito, J. Fraissard, J. Chem. Soc., Faraday Trans. 1 78 (1982) 403–410.
[13] D. Raftery, B.F. Chmelka, in: P. Kosfeld, B. Blumich (Eds.), NMR Basic Principles and Progress, vol. 30, Springer-Verlag, Berlin, 1994, pp. 111–158.
[14] M. Boudart, L.C. de Ménorval, G.P. Valenca, J. Phys. Chem. 92 (1988) 4033–4035.
[15] L. Itani, Y. Liu, W. Zhang, K.N. Bozhiliv, L. Delmotte, V. Valtchev, J. Am. Chem. Soc. 131 (2009) 10127–10139.
[16] R. Ryoo, C. Pak, D.H. Ahn, L.C. de Ménorval, F. Figueras, Catal. Lett. 7 (1990) 417–422.
[17] T. Ito, L.C. de Ménorval, E. Guerrier, J. Fraissard, Chem. Phys. Lett. 111 (1984) 271–274.
[18] E. Trescos, F. Rachdi, L.C. de Ménorval, F. Fajula, T. Nunes, G. Feio, J. Phys. Chem. 97 (1993) 11855–11857.
[19] B.F. Chmelka, D. Raftery, A.V. Mcormick, L.C. de Ménorval, R.D. Levine, A. Pines, Phys. Rev. Lett. 66 (1991) 580–583.
[20] L.C. de Ménorval, D. Raftery, S.B. Liu, K. Takegoshi, R. Ryoo, A. Pines, J. Phys. Chem. 94 (1990) 27–31.
[21] G. Fetter, D. Tichit, L.C. de Ménorval, F. Figueras, Appl. Catal. 65 (1990) L1–L4.
[22] M.A. Springuel-Huet, K. Sun, J. Fraissard, Micropor. Mesopor. Mater. 33 (1999) 89–95.
[23] A. Galarneau, H. Cambon, T. Martin, L.C. de Ménorval, D. Brunel, F. Di Renzo, F. Fajula, Stud. Surf. Sci. Catal. 141 (2002) 395–402.
[24] M.-A. Springuel-Huet, J.L. Bonardet, A. Gedeon, Y. Yue, V.N. Romannikov, J. Fraissard, Micropor. Mesopor. Mater. 44–45 (2001) 775–784.
[25] V.V. Terskikh, I.L. Moudrakovski, S.R. Breeze, S. Lang, C.I. Raadcliffe, J.A. Ripmeester, A. Sayari, Langmuir 18 (2002) 5653–5656.
[26] A. Gedeon, J.L. Bonardet, J. Fraissard, J. Phys. Chem. 97 (1993) 4254–4255.
[27] R. Ryoo, H. Ihee, J.H. Kwak, G. Seo, S.B. Liu, Micropor. Mater. 4 (1995) 59–64.
[28] F. Chen, F. Deng, M. Cheng, Y. Yue, C. Ye, X. Bao, J. Phys. Chem. B 105 (2001) 9426–9432.
[29] S.J. Huang, Q. Zhao, W.H. Chen, X. Han, X. Bao, P.S. Lo, H.K. Lee, S.B. Liu, Catal. Today 97 (2004) 25–34.
[30] A.K. Jameson, C.J. Jameson, H.S. Gutowsky, J. Chem. Phys. 53 (1970) 2310–2321.